FAST FIELD CYCLING NMR RELAXOMETRY

from molecular dynamics
to practical applications

STELAR

/INDEX

Contents

1	INTRODUCTION:	03
1.1	THE FAST FIELD CYCLING (FFC) NMR RELAXOMETRY TECHNIQUE	03
1.2	FFC AND MOLECULAR DYNAMICS	04
2	INSTRUMENTATION: FFC NMR INSTRUMENTS	04
3	FFC NMR APPLICATIONS:	06
3.1.1	MRI CONTRAST AGENTS	06
3.1.2	RECENT ACHIEVEMENT AND INNOVATIONS: PRELIMINARY STUDY OF A NEW IN-VIVO APPLICATION: FFC-NMRD PROFILES OF TUMOUR-BEARING MOUSE LEG	07
3.2	THERAPEUTIC PROTEINS	09
3.3	FOOD	11
3.4	POLYMERS	13
3.5	POROUS MATERIALS AND OIL INDUSTRY	15
3.6	HETERONUCLEI	17

1.1

/INTRODUCTION: FAST FIELD CYCLING RELAXOMETRY (FFC)

The Fast Field Cycling (FFC) NMR Relaxometry technique

Field Cycling NMR relaxometry is the only low-field NMR technique which measures the longitudinal spin relaxation rate, $1/T_1$, as a function of the magnetic field strength, over a wide range of frequencies (from a few kHz to 42 MHz (1 Tesla) or higher with the limitation being the size of the magnet and the FC technique being used), corresponding to values of T_1 in the order of seconds to a fraction of a millisecond. This can be done by using a single instrument with a magnet capable of fast eletrical switching of the field (also known as Fast Field Cycling (FFC)), which is commercially available, or through home-built systems which involve physically moving the sample between different magnets or within the stray magnetic field of a high field magnet, known as *shuttling* [1-6, 13].

The data can be displayed in the form of a nuclear magnetic resonance dispersion (NMRD) profile, $R_1(\omega) = 1/T_1(\omega)$ versus the field frequency (measured in MHz) [1, 7, 10-12].

Fast field cycling NMR relaxometry is the only technique which permits the measurement of nuclear spin relaxation times over a wide range of magnetic field strengths with just one instrument, thus offering a more complete investigation of molecular dynamics in a variety of substances and materials.

Examples of NMRD profiles for a range of different applications are described herein.

1.2

/INTRODUCTION: FAST FIELD CYCLING RELAXOMETRY (FFC)

FFC NMR and molecular dynamics

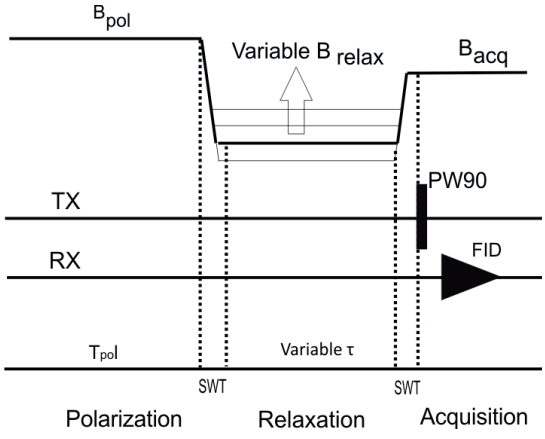

FIG. 1: *schematic representation of the field cycling technique.*

The spin-lattice (or longitudinal) relaxation time T_1, when studied over a wide range of magnetic field strengths, can furnish important information on molecular dynamics (motions) of water molecules in a variety of different environments.

The spin-lattice (or longitudinal) relaxation time T_1 when studied over a wide range of magnetic field strengths, can furnish important information on molecular dynamics (motions) of water molecules in a variety of different environments.

Unlike optical spectroscopy, spin relaxation is not spontaneous, but driven by fluctuating fields created by the molecular dynamics in the sample. Generally, molecular motions change the relative positions of nuclear and electron spins at the rates of molecular rotation and translation which create the stimulation for spin relaxation. The spin relaxation rate constant $1/T_1$ is proportional to the spectral density function evaluated at ω - the Larmor frequency - and 2ω. The spectral density is Fourier transform of the time-correlation function that characterizes the molecular motions [1, 13-15]. Therefore, measuring the relaxation rate constant as a function of ω or magnetic field strength provides a fundamental characterization of the molecular dynamics present in the system, including translational and rotational motions and chemical exchange events. A critical feature of the measurement is that the dynamics may be studied to frequencies as low as 10 kHz, which is very low compared with other spectroscopic approaches.

The technical problem is that the signal strength is proportional to the field; lowering the field lowers the signal.

A field cycle (**FIG. 1**) overcomes the pro-blem and permits rapid acquisition of the ma- gnetic field dependence of the spin relaxation rate. The field is switched on to a high value to polarize the spins, then switched to a relaxation field in which they relax for a variable time, then switched to a detection field where the magnetization is sampled. The process is repeated automatically for different relaxation evolution times and different fields to generate the relaxation dispersion profile that is a map of the molecular dynamics spectrum.

2 / INSTRUMENTATION

FFC NMR instruments

FIG. 2A: *Picture of the first SPINMASTER 0.5 T, installed at the University of Lund, Sweden, in 1997.*

Commercial FFC NMR relaxometers have been available since 1997.

They exploit the principle that the nuclear spin-lattice relaxation, T_1 is dependent on the magnetic field strength, as shown by very early works [8, 9, 12, 13]. The NMRD profile is obtained by switching the current very rapidly in a dedicated multi-section magnet. The field switched system permits measurement of relaxation rate constants approximately 100 times shorter than sample shuttle instruments and thus open a very wide range of experimental possibilities [1-4, 6-7].

The first commercial FFC relaxometer, from Stelar Srl (Mede, Italy), was installed at the University of Lund in 1997 (**FIG. 2A**) and operated with a two-layer air-core solenoid magnet

FIG. 2B:
1T SPINMASTER.

FIG. 2C:
Bench-top 0.25 T SMARtracer.

FIG. 2D:
Variable cryogen free HT superconducting magnet (HTS-100, NZ).

which achieved magnetic fields from 10kHz to 20 MHz.

The current version of the SPINMASTER (**FIG. 2B**) operates with a 1 Tesla four-layer air core solenoid magnet, capable of achieving fields from a few kHz (1-10 kHz is achievable depending on the local environment and field) to 42 MHz. SPINMASTER can also be configured with a 0.5 Tesla wide-bore magnet for 1 inch samples. The bench-top 0.25 T FFC relaxometer from Stelar (**FIG. 2C**) covers a field range from 10 kHz to 10 MHz. It is also possible to extend the field range of FFC relaxometers, up to 125 MHz, using a secondary variable-field magnet in conjunction with the FFC system (**FIG. 2D**).

Commercial FFC NMR relaxometers have been available from Stelar since 1997.

REFERENCES:

[1] Kimmich R., Anoardo, E., (2004), *Field-Cycling NMR Relaxometry*, Progress in Nuclear Magnetic Resonance Spectroscopy, *44*, 257-320;
[2] Redfield A.G., (2003), *Shuttling device for high-resolution measurements of relaxation and related phenomena in solution at low field, using a shared commercial 500 MHz NMR instrument.* Magn Reson Chem., *41*, 753–768;
[3] Redfield A. G., (2012), *High-resolution NMR field-cycling device for full-range relaxation and structural studies of biopolymers on a shared commercial instrument*. Journal of biomolecular NMR, *52(2)*, 159-177;
[4] Job C., Zajicek J., Brown M.F., (1996), *Fast field-cycling nuclear magnetic resonance spectrometer*, Rev. Sci. Instrum., *67 (6)*, 2113-2122;
[5] Wagner S., Dinesen T.R.J., Rayner T., Bryant R.G., (1999) , *High-resolution magnetic relaxation dispersion measurements of solute spin probes using a dual-magnet system*, J. Magn. Reson., *140*, 172-178;
[6] Victor K., Kavelius V., Bryant R.G., (2004), *Magnetic relaxation dispersion probe*, J. Magn. Reson., *171(2)*, 253-257;
[7] Ferrante G., Sykora S., (2005), *Technical aspects of Fast-Field Cycling*, Advances in Inorganic Chemistry, *57*, 405-470;
[8] Ramsey N.F., Pound R.V., (1950), *Nuclear Audiofrequency Spectroscopy by Resonant Heating of the Nuclear Spin System*, Phys. Rev., *77*, 278-279;
[9] Abragam A., (1961), *The principles of Nuclear Magnetism*, Clarendon Press, Oxford;
[10] Fujara E., Kruk D., Privalov A.F., (2014), *Solid state Field-Cycling NMR relaxometry: Instrumental improvements and new applications*. Progress in nuclear magnetic resonance spectroscopy, 82, 39-69
[11] Steele, R. M. , Korb, J. P., Ferrante, G. , Bubici S., (2015) *New applications and perspectives of fast field cycling NMR relaxometry*. Magnetic Resonance in Chemistry, *54(6)*, June 2016, 502–509;
[12] Noack F. (1986), *NMR field-cycling spectroscopy: principles and applications*. Progress in nuclear magnetic resonance Spectroscopy, *18(3)*, 171-276;
[13] Kimmich, R. (1980), *Field cycling in NMR relaxation spectroscopy: applications in biological, chemical and polymer physics*, Bull. Magn. Reson, 1(4), 195-218;
[14] McConnell, J. (2009). *The theory of nuclear magnetic relaxation in liquids*. Cambridge, UK: Cambridge University Press, 2009, 1;
[15] Slichter, C. P. (1990). *Elements of resonance*, in *Principles of magnetic resonance*, Springer: Berlin Heidelberg, 1-9.

/ APPLICATIONS

3.1.1 MRI contrast agents

FFC NMR technique allows investigation of the interaction between metal ions and water which can be used to improve the effectiveness of a contrast agent and to optimize its design.

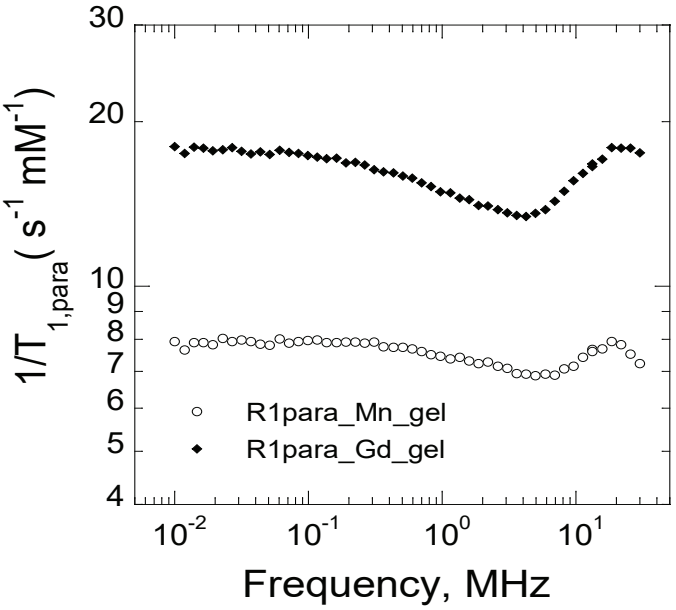

FIG. 3: *^{1}H NMRD profiles of Gadolinium and Manganese bovine serum albumin (BSA) cross-linked gels.*

Rapid progress has been made in developing new MRI contrast agents (paramagnetic complexes) as well as in the instrument technology to characterize the T_1 relaxivity profile (NMRD) of the agent. Contrast agents with higher relaxivity are more desirable as they enhance the relaxation of body tissues of interest in the MRI scan.

Research has led to the development of MRI-trackable magnetic nanoparticles capable of targeting specific cell-types, such as cancer cells, for image-guided treatment [1, 2, 5, 8].

NMRD is critical for characterizing the mechanistic origins of contrast agent effects and mapping the magnetic field dependence of their magnetic relaxation efficiency. Relaxivity is the water-proton-relaxation rate normalized by the contrast agent concentration. Higher relaxivity permits reduction of agent concentration and reduced toxicity. Gadolinium(III), manganese(II) and iron (III) are the most frequently used metal centers because these S-state ions have large net electron spin moments and relatively long electron spin relaxation times. [6-11]

Parameters involved in relaxation can be estimated by fitting the NMRD profile of the contrast agent with an appropriate mathematical model relating to a particular theory.

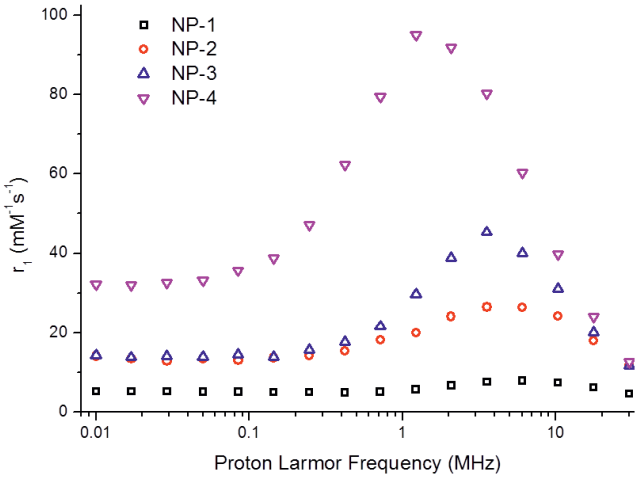

FIG. 4: *^{1}H NMRD profiles of magnetic iron oxide nanoparticles with increasing core sizes.*

- *4 nm (NP-1)*
- *6 nm (NP-2);*
- *9 (NP-3)*
- *14 nm (NP-4)*

NMRD profiles permit determination of what local dynamical factors dominate the nuclear spin relaxation detected. Three factors compete: rotational motion, chemical exchange, and electron spin relaxation with electron spin relaxation usually the limiting factor (FIG. 3 and FIG. 4).
In FIG. 3, the rotational motion has been stopped in the samples by crosslinking the bovine serum albumin to which the metals are bound.
The fast process that limits the relaxivity is the electron spin relaxation time which becomes the correlation time for the electron-nuclear coupling and it increases with increasing Larmor frequency causing the maximum in the relaxivity [3].
The water relaxivity for the 4 nm to 14 nm magnetic nanoparticle suspension shown in FIG. 4 are also limited by magnetic relaxation processes associated with the magnetic particles themselves which competes with translational motion of the water in the vicinity of the nanoparticles.
These data show that it is possible to tune the relaxivity to be optimal at different field strengths by altering and adjusting the size and composition of the nanoparticles [4].

/RECENT ACHIEVEMENTS AND INNOVATIONS

3.1.2 Study of a new in-vivo application: FFC-NMRD profiles of tumour-bearing mouse leg

The acquisition of in-vivo NMRD profiles on animal models is a fundamental step forward in validating the clinical effectiveness of FFC-MRI with the final goal of finding new biomarkers characterizing different diseases for an earlier diagnosis with lower costs and new protocols responsive to changes in water mobility following therapeutic treatment.

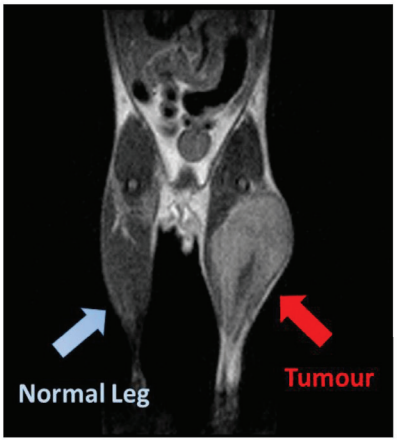

FIG. 5:
This MRI image shows the difference between normal and tumour-bearing mouse leg.

FIG. 6:
Mouse in the wide bore probe.

Many diseases are inadequately diagnosed, or not diagnosed early enough by current imaging methods. Examples of unmet clinical needs arise in thromboembolic disease, osteoarthritis, cancer, sarcopenia, and many more areas. As shown by clinical pilot studies [12-13], in-vivo Fast Field-Cycling (FFC) can provide completely new diagnostic information currently inaccessible to standard MRI operating at relatively high field. Indeed, FFC introduces an entirely new dimension into MRI, namely the strength of the applied magnetic field.
In this study, a dedicated surface coil and a suitable RF interface has been developed for the acquisition of in-vivo NMRD profiles on animal model (FIG. 5 and FIG. 6).

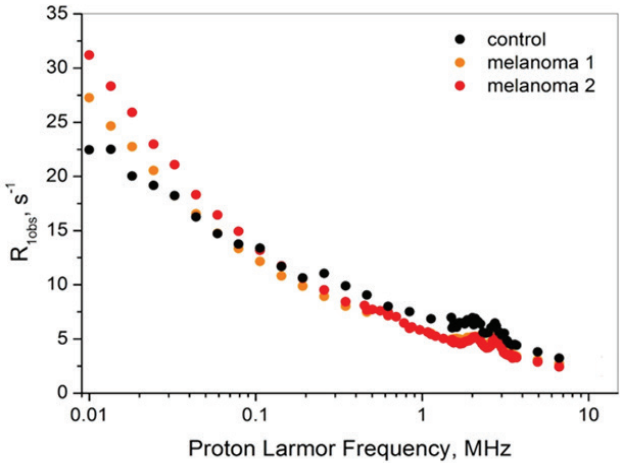

FIG. 7:
Melanoma tumours have shorter T_1 than normal tissue due to the higher iron content melanin aggregates. T_1 differences are proportional to the tumour size (132 and 180 mm^3 for tumour 1 and 2 rispectively).

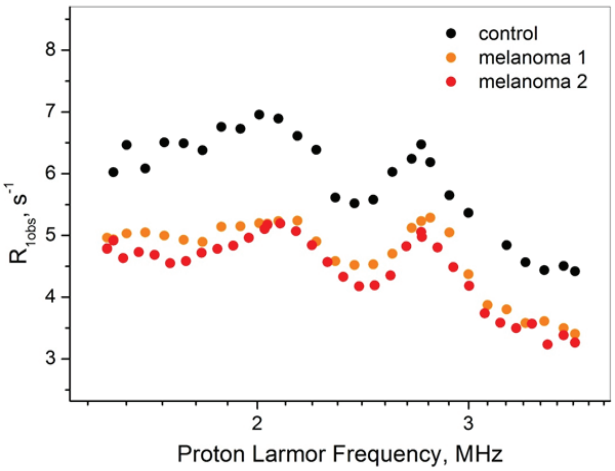

FIG. 8:
Quadrupolar peaks arising from protein amidic groups can be seen very clearly, centred at proton NMR frequencies of 0.65, 2.10 and 2.75 MHz. This is a phenomenon that is completely invisible to conventional (fixed-field) MRI but fully exploitable by FFC-NMR.

REFERENCES:

[1] Lévy M., Gazeau F., Wilhelm C., Neveu S., Devaud M., Levitz P., (2013), *Revisiting MRI Contrast Properties of Nanoparticles: Beyond the Superparamagnetic Regime,* J Phys Chem C., *117*, 15369–15374;
[2] De Cola C., Fiorillo G., Meli A., Aime S., Gianolio E., Izzo I., De Riccardis F., (2014), *Gadolinium-binding cyclic hexapeptoids: synthesis and relaxometric properties*, Org Biomol Chem., *12*, 424-431;
[3] Korb J.-P., Diakova G., Bryant R.G. (2006), *Paramagnetic relaxation of protons in rotationally immobilized proteins*, J. Chem. Phys., *124 (13)*, 134910;
[4] Boni A., Gemmi M., Innocenti C., Bardi G., Bertero A., Signore G., Bifone A., (2014), *Colloidal Nanoparticles for Biomedical Applications IX*, Eds. W. J. Parak, M. Osinski, K.I. Yamamoto, Proc. of SPIE, 8955, 895502-1 ;
[5] Arruebo M., Fernández-Pacheco R., Ibarra M. R., & Santamaría J. (2007). *Magnetic nanoparticles for drug delivery*. Nano today, *2(3)*, 22-32.
[6] Aime S., Botta M., & Terreno E. (2005). *Gd (III)-based contrast agents for MRI*. Advances in Inorganic Chemistry, *57*, 173-237.
[7] Chan K. W. Y., & Wong W. T. (2007). *Small molecular gadolinium (III) complexes as MRI contrast agents for diagnostic imaging*. Coordination Chemistry Reviews, *251(17)*, 2428-2451.
[8] Yan G. P., Robinson L., & Hogg P. (2007). *Magnetic resonance imaging contrast agents: overview and perspectives*. Radiography, *13*, e5-e19.
[9] Caravan P., Ellison J. J., McMurry T. J., & Lauffer R. B. (1999). *Gadolinium (III) chelates as MRI contrast agents: structure, dynamics, and applications*. Chemical reviews, *99(9)*, 2293-2352.
[10] Caravan P., Farrar C. T., Frullano L., & Uppal R. (2009). *Influence of molecular parameters and increasing magnetic field strength on relaxivity of gadolinium-and manganese-based T_1 contrast agents*. Contrast media & molecular imaging, *4(2)*, 89-100.
[11] Casula M. F., Floris P., Innocenti C., Lascialfari A., Marinone M., Corti M., & Sangregorio C. (2010). *Magnetic resonance imaging contrast agents based on iron oxide superparamagnetic ferrofluids*. Chemistry of Materials, *22(5)*, 1739-1748;
[12] Broche LM., Ashcroft GP. & Lurie, DJ. (2012). '*Detection of osteoarthritis in knee and hip joints by fast field-cycling NMR*'. Magnetic Resonance in Medicine, vol 68, no. 2, pp. 358-362 ;
[13] Broche LM., Kennedy BW., MacEachern C., Ashcroft GP. & Lurie DJ. (2014). *Fast field-cycling NMR of cartilage: a way toward molecular imaging*. Osteoarthritis and Cartilage, vol 22, no. Supplement, pp. S66-S67.

/ APPLICATIONS

3.2 Therapeutic proteins

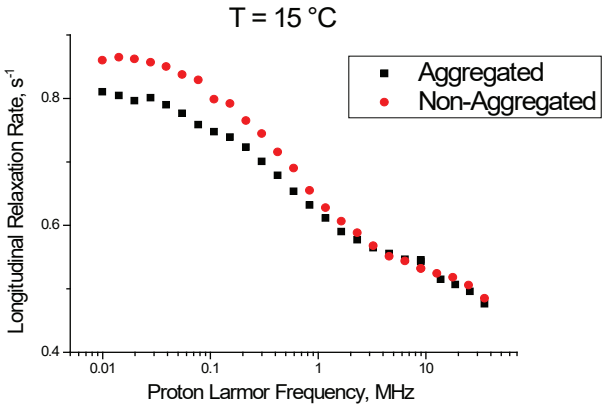

FIG. 9:
^{1}H NMRD profiles of a therapeutic monoclonal antibody in its monomeric (non-aggregated) and an artifcially aggregated states.

The aggregation of therapeutic proteins is an important issue in the bio-pharmaceutical industry. FFC NMR Relaxometry shows considerable promise for making routine assessments of therapeutic protein aggregation and denaturation.

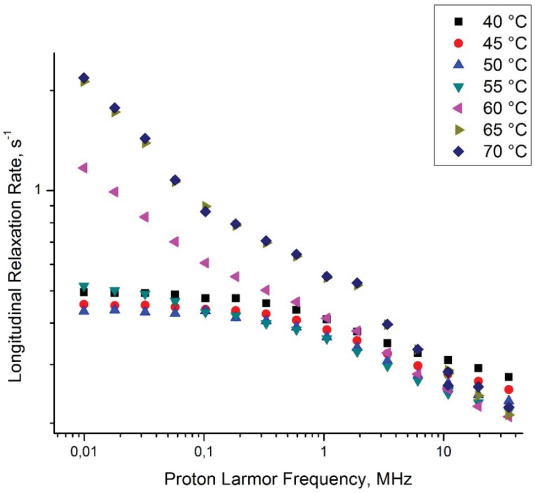

FIG. 10:
^{1}H NMRD profiles of a monomeric therapeutic protein at different temperatures corresponding to unfolding dynamics.

The aggregation of therapeutic proteins (e.g. monoclonal antibodies) is an important problem in the bio-pharmaceutical industry. It is well documented that protein product aggregates are potent inducers of immune responses to therapeutic protein products, thus manufacturers of therapeutic protein products should ensure that their products contain minimal product aggregates.

Currently size exclusion chromatography (SEC) is primarily used in combination with orthogonal methods to confirm aggregate sizes present. There is a real need for new and improved analytical methods for defining protein aggregates for the benefit of the patient, to avoid constraining the production capacity of therapeutic proteins over the coming years and to prevent loss of therapeutic proteins through aggregation during the manufacturing process and storage [1,2]. FFC NMR relaxometry shows considerable promise for making routine assessments of protein aggregation and denaturation.

The unique feature of NMRD is that it can be used to characterize very large aggregates because of the very low frequencies achieved and does not suffer from aggregate fraction or separation as the system is measured [3]. **FIG. 9** shows the ^{1}H NMRD profiles of a therapeutic protein (10 mg/mL) in its monomeric «non-aggregated» state and with artificially induced aggregation [4]. The differences between the aggregated and non-aggregated states can be most clearly seen at lower magnetic field strengths.

Adoption of the FFC method for such an application in an industrial setting would not necessarily require the full NMRD profile but instead calibration at a few low field points.

The main asset of FFC is that it is non-destructive. **FIG. 10** shows how ^{1}H NMRD profiles can also show the dynamics in monomeric therapeutic proteins at different temperatures [4]. The temperature-dependent behaviour of one antibody (10 mg/mL) was studied between 40 °C and 70 °C. The protein initially aggregated (40-55 °C) then unfolded (above 55 °C). The unfolding behaviour is clear at low magnetic field strengths.

MAIN TOPICS CONCERNING PROTEIN NMRD PROFILES

- to investigate the level of aggregation in proteins or proteins mixture;
- to assess changes in protein aggregation;
- to study protein-protein interactions;
- to obtain information concerning molecular dynamics of proteins ;
- to study protein changes due to a change of solution temperature;
- to obtain the 'fingerprinting' of a certain protein;
- to evaluate the size distribution of a certain protein species;
- to estimate the degree of hydration of a protein;
- to estimate the protein concentration in a solution ;
- to quantify different protein species in a mixture.

REFERENCES:

[1] Shacter E., CHI meeting, April 4 2011, Bethesda, MD, USA;
[2] Rosenberg A.S., (2006), *Effects of Protein Aggregates: An Immunologic Perspective*, The AAPS journal, *8(3)*, article 59;
[3] Diakova G., Goddard Y.A., Korb J.-P., Bryant R.G., (2010), Biophysical Journal, *98*, 138–146;
[4] Data from in-house studies at Stelar.
[5] Borsi V., Luchinat C., & Parigi G. (2009). *Global and local mobility of apocalmodulin monitored through fast-field cycling relaxometry*. Biophysical journal, *97(6)*, 1765-1771.
[6] Bertini I., Gupta Y. K., Luchinat C., Parigi G., Schlörb C., & Schwalbe H. (2005). *NMR spectroscopic detection of protein protons and longitudinal relaxation rates between 0.01 and 50 MHz*. Angewandte Chemie International Edition, *44(15)*, 2223-2225.
[7] Luchinat C. & Parigi G. (2007). *Collective relaxation of protein protons at very low magnetic field: a new window on protein dynamics and aggregation*. Journal of the American Chemical Society, *129(5)*, 1055-1064.
[8] Berti F., Costantino P., Fragai M., & Luchinat C. (2004). *Water accessibility, aggregation, and motional features of polysaccharide-protein conjugate vaccines*. Biophysical journal, *86(1)*, 3-9.
[9] Gottschalk M., Nilsson H., Roos H., & Halle B. (2003). *Protein self-association in solution: The bovine β-lactoglobulin dimer and octamer*. Protein Science, *12(11)*, 2404-2411.
[10] Snoussi K., & Halle B. (2005). *Protein self-association induced by macromolecular crowding: a quantitative analysis by magnetic relaxation dispersion*. Biophysical journal, *88(4)*, 2855-2866.

/ APPLICATIONS

3.3 Food

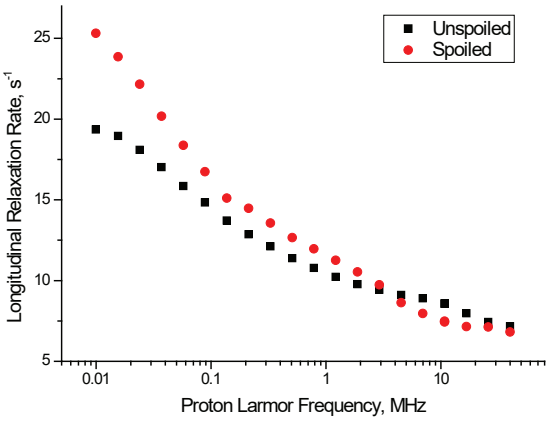

FIG. 11: *^{1}H NMRD profiles of an unbranded milk-based refrigerated drink product before and after artificial spoilage (acidification).*

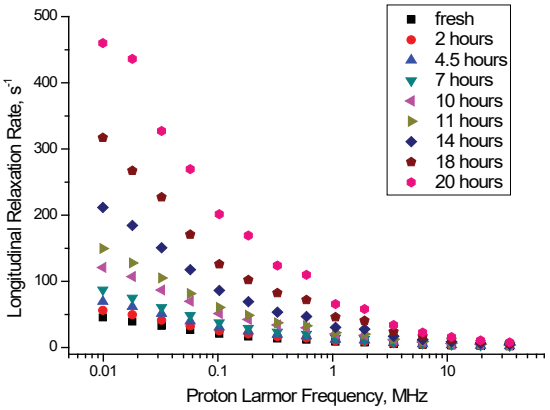

FIG. 12: *^{1}H NMRD profiles of pork loin open to air at ambient temperature over a twenty hour time period.*

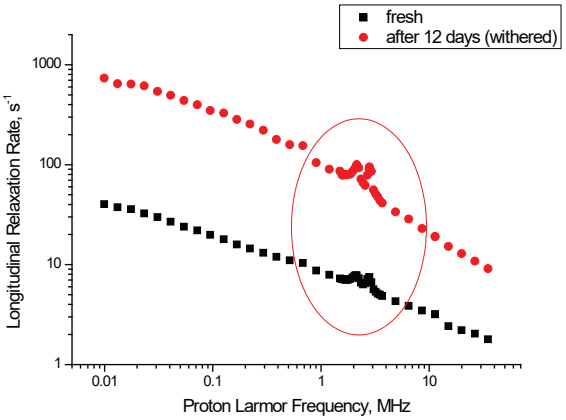

FIG. 13: *^{1}H NMRD profiles of pork loin open to air at ambient temperature over 12 days.*

Food is a complex matrix for which NMRD has shown diagnostic utility. The NMRD profile is sensitive to dehydration, oxidation, spoilage, and the addition of additives including adulterants that may lead to fraudulent products [1-3, 6-10].

MILK-BASED PRODUCTS

Milk sours when bacterial fermentation transforms the sugars to lactic acid. Acid may denature proteins present and drive protein aggregation both of which affect the NMRD profile. Fermentation may be monitored by relaxometry, and spoilage monitored as shown in **FIG. 11** for a refrigerated drink product [4]. In these cases, low magnetic field measurements are a critical advantage, and the profile shape is diagnostic.

MEAT

Meat has a short shelf-life and thus needs to be stored rigorously at cold temperatures. NMRD can show how quickly meat, such as the pork loins shown in **FIG. 12**, can dehydrate over a period of 20 hours [4]. After 12 days the pork loins have lost a lot of water (as shown by the NMRD in **FIG. 13**) [4].

A more detailed analysis of **FIG. 13** reveals quadrupolar dips or peaks in both NMRD: this phenomenon is due to magnetization transfer from water protons to ^{14}N nuclei at a short range, leading to an increase in water proton relaxation [5]. This occurs when one of the nuclear quadrupolar energy levels matches the ^{1}H Larmor frequency thus producing the quadrupolar dips/peaks observed in the NMRD profile.

Quadrupolar dips/peaks are generally only observed in solids, gels and liquid crystals, where the NH bond is sufficiently immobilized. In this case (**FIG. 13**) the quadrupole peaks are due to the immobilized proteins in the meat.

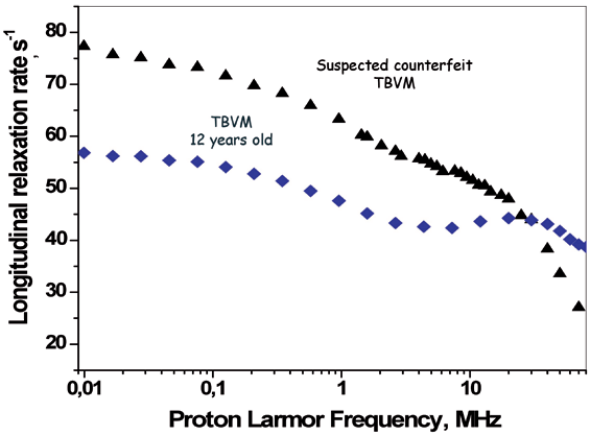

FIG. 14:
NMRD profiles for 12yrs aged balsamic vinegar (blue) and counterfeit product (black).

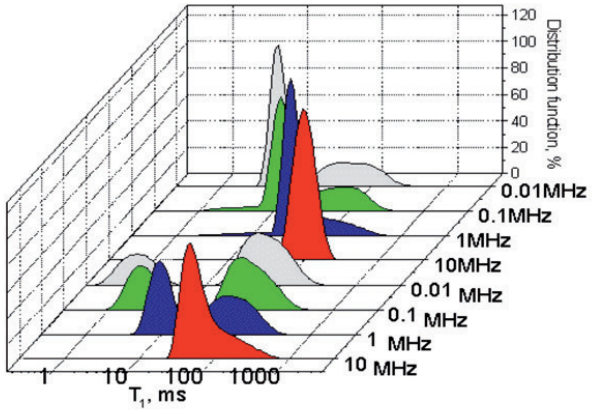

FIG. 15:
T_1 distributions of Parmesan cheese taken from parts of the crust and of the core obtained using an inverse Laplace algorithm.

BALSAMIC VINEGAR (ITALIAN)
NMRD profiles have been applied for characterizing the age of balsamic vinegar (TBVM, FIG. 14, [2]). TBVM is a protected designation of origin product and its cost on the market is rather high in accordance with its ageing process.

PARMESAN CHEESE (ITALIAN)
FFC NMR has applied to characterize high quality italian Parmesan cheese produced following strict criteria (FIG.15, from house-made data).

REFERENCES:

[1] Capitani D., Sobolev A.P., Delfini M., Vista S., Antiochia R., Proietti N., Bubici S., Ferrante G., Carradori S., De Salvador F. R., Mannina L., (2014), *NMR methodologies in the analysis of blueberries*, Electrophoresis, *35(11)*, 1615–1626;
[2] Baroni S., R. Consonni, G. Ferrante, S. Aime, (2009), *Relaxometric studies for food characterization: the case of balsamic and traditional balsamic vinegars*, J Agric Food Chem., *57(8)*, 3028-32;
[3] Curti E.,Bubici S.,Carini E., S. Baroni S., Vittadini E., (2011), *Water molecular dynamics during bread staling by Nuclear Magnetic Resonance*, LWT - Food Science and Technology, *44(4)*, 854-859;
[4] Data from in-house studies at Stelar;
[5] Broche L.M., Ismail S.R., Booth N.A., Lurie D.J., (2012), *Measurement of fibrin concentration by fast field-cycling NMR*, Magnetic Resonance in Medicine, *67(5)*, 1453–1457;
[6] Conte, P., Mineo, V., Bubici, S., De Pasquale, C., Aboud, F., Maccotta, A., & Alonzo, G. (2011). *Dynamics of pistachio oils by proton nuclear magnetic resonance relaxation dispersion.* Analytical and bioanalytical chemistry, *400(5)*, 1443-1450;
[7] Rachocki A., & Tritt-Goc J. (2014). *Novel application of NMR relaxometry in studies of diffusion in virgin rape oil*, Food chemistry, *152*, 94-99;
[8] Godefroy S., Korb J. P., Creamer L. K., Watkinson P. J., & Callaghan P. T. (2003). *Probing protein hydration and aging of food materials by the magnetic field dependence of proton spin-lattice relaxation times.* Journal of colloid and interface science, *267(2),* 337-342;
[9] Baroni S., Consonni R., Ferrante G., & Aime S. (2009). *Relaxometric studies for food characterization: the case of balsamic and traditional balsamic vinegars.* Journal of agricultural and food chemistry, *57(8)*, 3028-3032
[10] Laghi L., Cremonini M. A., Placucci G., Sykora S., Wright K., & Hills B. (2005). *A proton NMR relaxation study of hen egg quality*. Magnetic resonance imaging, *23(3)*, 501-510.

/ APPLICATIONS

3.3 Polymers

There are several interesting applications for polymer characterization which are potentially applicable to the polymer industry and that could be developed to become standard analytical tools.

FFC NMR relaxometry has frequently been employed to solve problems in characterization of complex materials [21-27], including polymers [1-3, 7-17].

As shown in **FIG. 16**, FFC NMR technique can be used for polymers fingerprinting, due to the fact that the molecular dynamics of these systems presents very different behavior, which is reflected in their NMR dispersion profiles. From **FIG. 17**, it is also evident that, at low fields, it is easier to discriminate between different kinds of polymers.

Small differences in the composition/structure of some polymers may lead to large differences in the desired physical/mechanical properties and thus it is important to be able to differentiate between these .

Small deviations in manufacturing procedure may lead to a polymer product not meeting the required performance parameters.

FIG. 17 shows an example of how FFC can be used to distinguish between two samples of the same polymer, made at two different manufacturing sites [4].

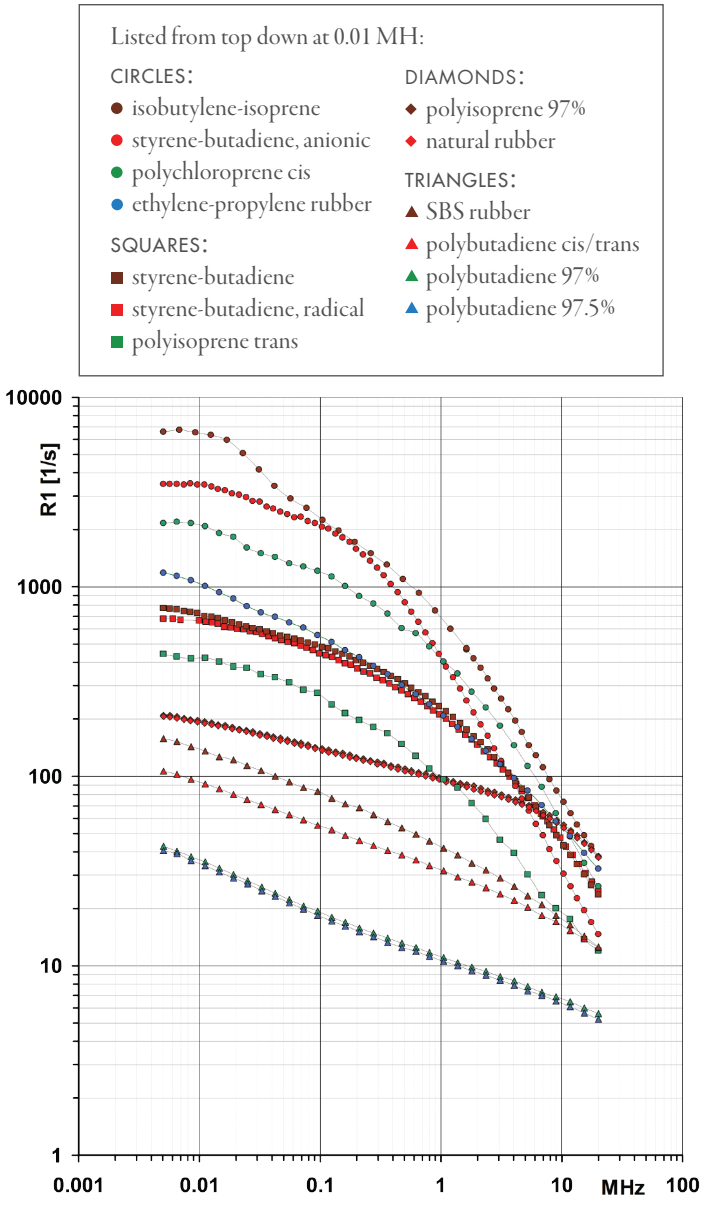

FIG. 16: *NMRD profiles of different polymers from 0.005 MHz to 20 MHz. From in-house data.*

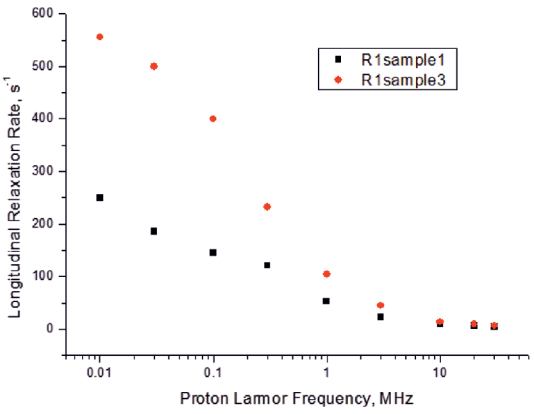

FIG. 17: *^{1}H NMRD profiles of two identical polymers produced by two different manufacturing sites which displayed different mechanical properties.*

These polymers showed different mechanical properties. The ^{1}H NMRD profiles of the two polymer samples revealed large differences in $1/T_1$ at low magnetic field strengths, which were not revealed at the higher magnetic field strengths at which many permanent magnet (fixed field) relaxometers work (e.g. 5 or 20 MHz). Moreover, FFC NMR is very useful to investigate chain dynamics in entangled polymer systems and polymer melts [28] and can be also applied to study molecular order (dynamics slows down when the molecular weight is increased) and inter-segment interactions [29, 30]. Furthermore, there are interesting applications for polymer characterization which are exploitable by the polymer industry and that could be developed to become standard analytical tools. Polymeric chains present dynamic processes not present in other compounds which are strongly correlated to the macroscopic mechanical properties of the materials. From a comparison with rheological studies FFC NMR emerges as method of molecular rheology (**FIG. 18**) to be applied to polymers, rubbers and dendrimers for which all rheological changes are reflected in the FFC dispersion curves [9,12]. This information can be exploited to control polymer melt processing in industry. The dynamics of polymers has huge practical interest due to the fact that most plastic objects are made from melts. ■

FFC NMR technique emerges as method of molecular rheology.

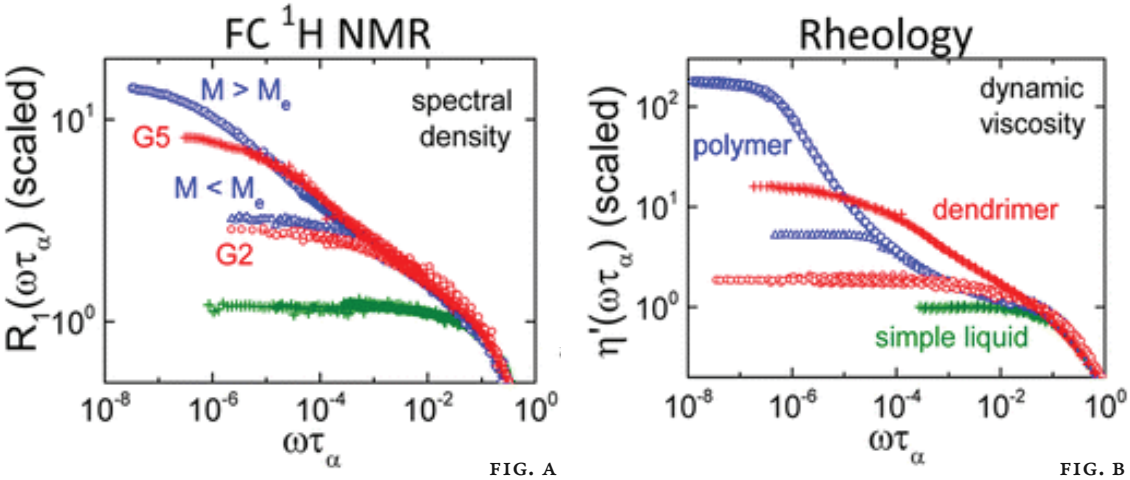

FIG. A FIG. B

FIG. 18:
Results from PPG (polypropylene glycol) and PPI (polypropyleneimine) dedrimers with different molar masses (M) investigated with FFC ^{1}H NMR, shear rheology (G) and dielectric spectroscopy (DS).
Results are compared in a reduced spectral density representation.
The picture on the left (FIG. A) represents the master curve of $R_1(\omega\tau_\alpha)$ with τ_α indicating the local correlation time.
The picture on the right (FIG. B) is instead the rescaled dynamic viscosity $\eta'(\omega\tau_\alpha)$. The close correspondence of these two functions makes the FFC NMR technique a powerful tool of molecular rheology allowing to investigate the microscopical processes behind the macroscopical rheological behavior of complex fluids (adapted from [12]).

/ APPLICATIONS

3.4 Porous materials and oil industry

With crude oil reserves diminishing, it is increasingly important to extract the maximum yield of oil possible from the reservoir. Injecting various aqueous preparations is one method used to force oil to the surface.

Geological factors of importance include the type of reservoir rock, its porosity and its wettability. In rocks with small pores, wettability is a key factor for assessment of oil extraction.

FFC NMR can be used to determine pore size distribution in porous rocks containing petroleum.

Understanding the dynamics and transport properties of water and crude oil in porous rocks is crucial for the petroleum industry to improve the extraction processes and yields of crude oil.

The higher the wettability (or ***dynamical surface affinity***) the higher the probability that water can displace oil at the pore surface and thus the result should be a higher yield of oil [5, 6, 18, 19, 28].

In a study of three samples of carbonate rocks (S40, S50, S122; 1 inch diameter rock cores studied on a dedicated 0.5 T wide bore SPINMASTER FFC relaxometer) saturated with water, data from ^{1}H NMRD was used to assess the dynamical surface affinity of water (or wettability, **FIG. 19**) and the distribution of pore sizes (porosity) [4].

It was found that the dynamical surface affinity depends critically on the pore size. In **FIG. 20** the T_1 distributions of the 3 rocks at 0.01MHz are reported. ■

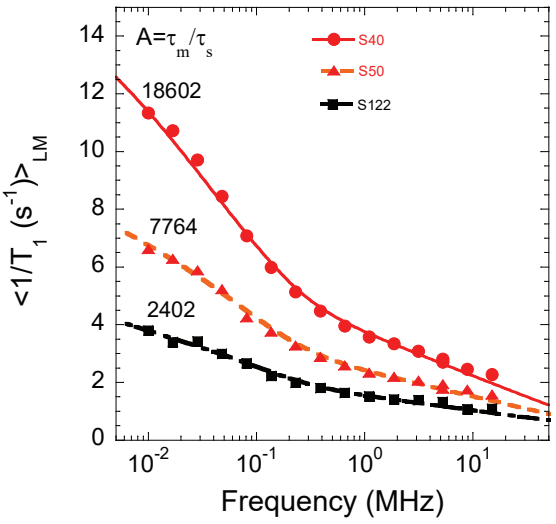

FIG. 19:
NMRD of the logarithmic average $<1/T_1>$ of 3 carbonate 1" rock cores. The consideration of such a logarithmic average allows quantitative comparison of the different NMRD data. The continuous lines are the best fits obtained with a bi-logarithmic surface relaxation model.
The dynamical surface affinity index, A, representing the local NMR wettability is given above each fit.

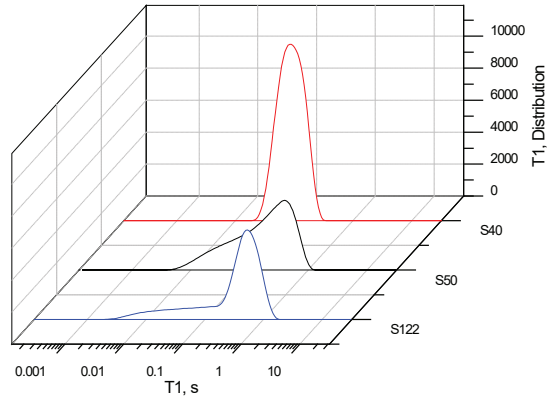

FIG. 20:
T_1 distributions of 3 carbonate rock core samples at 0.01 MHz.

REFERENCES:

[1] Kariyo S., Brodin A., Gainaru C., Herrmann A., Hintermeyer J., Schick H., Novikov V. N. & Rössler E. A., (2008), *From Simple Liquid to Polymer Melt. Glassy and Polymer Dynamics Studied by Fast Field Cycling NMR Relaxometry: Rouse Regime, Macromolecules, 41(14), 5322–5332*;
[2] Gubaidullin A., Shakirov T., Fatkullin N., Kimmich R., *Spin-lattice relaxation dispersion in polymers: dipolar-interaction components and short- and long-time limits*, Solid State Nucl Magn Reson., 2009, *35(3)*, 147-51;
[3] Fatkullin N., Gubaidullin A., Stapf S., (2010), *Features of polymer chain dynamics as revealed by intermolecular nuclear magnetic dipole-dipole interaction: Model calculations and field-cycling NMR relaxometry*, J. Chem. Phys., *132(9)*, 094903-1 – 094903-17;
[4] Data from in-house studies at Stelar;
[5] Korb J.-P., Freiman G., Nicot B., Ligneul P., (2009), *Dynamical surface affinity of diphasic liquids as a probe of wettability of multimodal porous media,* Physical Review E, *80*, 061601-1 – 061601-12;
[6] Korb J-P., Louis-Joseph A., Benamsili L., (2013), *Probing Structure and Dynamics of Bulk and Confined Crude Oils by Multiscale NMR Spectroscopy, Diffusometry, and Relaxometry*, J Phys Chem B., *117(23)*, 7002-7014;
[7] Kruk D., Hermann A., Rössler E.A., (2012), *Field-cycling NMR relaxometry of viscous liquids and polymers*, Progress in nuclear magnetic resonance spectroscopy, *63*, 33-64;
[8] Rössler E.A., Stapf S., Fatkullin N., (2013), *Recent NMR investigations on molecular dynamics of polymer melts in bulk and in confinement*, Current Opinion in Colloid & Interface Science, *18(3)*, 173-182;
[9] Meier R., Kruk D., & Rössler E. A., (2013), I*ntermolecular Spin Relaxation and Translation Diffusion in Liquids and Polymer Melts: Insight from Field-Cycling ^{1}H NMR Relaxometry*. ChemPhysChem, *14(13)*, 3071-3081;
[10] Hofmann M., Kresse B., Privalov A. F., Willner L., Fatkullin N., Fujara F., & Rössler E. A., (2014). *Field-Cycling NMR Relaxometry Probing the Microscopic Dynamics in Polymer Melts*. Macromolecules, *47(22)*, 7917-7929;
[11] Kresse B., Hofmann M., Privalov A. F., Fatkullin N., Fujara F., & Rössler E. A., (2015). *All Polymer Diffusion Regimes Covered by Combining Field-Cycling and Field-Gradient ^{1}H NMR*. Macromolecules, *48(13)*, 4491-4502;
[12] Hofmann M., Gainaru C., Cetinkaya B., Valiullin R., Fatkullin N., & Rössler E. A., (2015), *Field-Cycling Relaxometry as a Molecular Rheology Technique: Common Analysis of NMR, Shear Modulus and Dielectric Loss Data of Polymers vs Dendrimers,* Macromolecules, *48(20)*, 7521-7534;
[13] Fatkullin N., Stapf S., Hofmann M., Meier R. & Rössler E. A., (2015), *Proton spin dynamics in polymer melts: New perspectives for experimental investigations of polymer dynamics*, Journal of Non-Crystalline Solids, *407*, 309-317;
[14] Schmidtke B., Hofmann M., Lichtinger A. & Rossler E. A., (2015), *Temperature dependence of the segmental relaxation time of polymers revisited,* Macromolecules, *48(9)*, 3005-3013;
[15] Hofmann M., Kresse B., Heymann L., Privalov A. F., Willner L., Fatkullin N., Aksel N., Fujara F. & Rössler E. A., (2016), *Dynamics of a Paradigmatic Linear Polymer: A Proton Field-Cycling NMR Relaxometry Study on Poly (ethylene–propylene)*, Macromolecules, *49(22)*, 8622–8632;
[16] Lozovoi A., Mattea C., Herrmann A., Rössler E. A., Stapf S. & Fatkullin N., (2016), *Communication: Proton NMR dipolar-correlation effect as a method for investigating segmental diffusion in polymer melts*. The Journal of Chemical Physics, *144(24)*, 241101;
[17] Flämig M., Becher M., Hofmann M., Körber T., Kresse B., Privalov A. F. & Rössler E. A., (2016), *Perspectives of Deuteron Field-Cycling NMR Relaxometry for Probing Molecular Dynamics in Soft Matter*, The Journal of Physical Chemistry B, *120(31)*, 7754-7766;
[18] Korb J. P., (2010). *Multi-scales nuclear spin relaxation of liquids in porous media*. Comptes Rendus Physique, *11(2)*, 192-203;
[19] Korb J. P., (2011). *Nuclear magnetic relaxation of liquids in porous media*. New Journal of Physics, *13(3)*, 035016;
[20] Muncaci S., Mattea C., Stapf S., Ardelean I., (2013), *Frequency-dependent NMR relaxation of liquids fined inside porous media containing an increased amount of magnetic impurities*, Magnetic Resonance in Chemistry, *51(2)*, 123-128;
[21] Conte P. & Alonzo, G. (2013), *Environmental NMR: Fast-field-cycling Relaxometry*. eMagRes., *2(3)*, 389–398;
[22] Conte P., Marsala V., De Pasquale C., Bubici S., Valagussa M., Pozzi A. & Alonzo, G., (2013). *Nature of water-biochar interface interactions.* GCB Bioenergy, *5(2)*, 116-121;
[23] Badea C., Pop A., Mattea C., Stapf S. & Ardelean I., (2014), *The effect of curing temperature on early hydration of gray cement via fast field cycling-NMR relaxometry,* Applied Magnetic Resonance, *45(12)*, 1299-1309;

[24] Dalas F., Korb J. P., Pourchet S., Nonat A., Rinaldi D. & Mosquet M., (2014), *Surface relaxivity of cement hydrates*, The Journal of Physical Chemistry C, *118(16)*, 8387-8396;
[25] Bortolotti V., Brizi L., Brown R. J., Fantazzini P. & Mariani M., (2014), *Nano and Sub-nano Multiscale Porosity Formation and Other Features Revealed by ^{1}H NMR Relaxometry during Cement Hydration*. Langmuir, *30(36)*, 10871-10877;
[26] Conte P., Hanke U. M., Marsala V., Cimo, G., Alonzo G. & Glaser B., (2014), *Mechanisms of water interaction with pore systems of hydrochar and pyrochar from poplar forestry waste*, Journal of agricultural and food chemistry, *62(21)*, 4917-4923;
[27] Korb J. P., Nicot B., Louis-Joseph A., Bubici S. & Ferrante G., (2014), *Dynamics and wettability of oil and water in oil Shales*, The Journal of Physical Chemistry C, *118(40)*, 23212-23218.
[28] Herrmann A., Kresse B., Wohlfahrt M., Bauer I., Privalov A.F., Kruk, D., Fatkullin N., Fujara F. & Rössler E.A. (2012). *Mean square displacement and reorientational correlation function in entangled polymer melts revealed by field cycling ^{1}H and ^{2}H NMR relaxometry*. Macromolecules, *45(16)*, 6516-6526.
[29] Herrmann A., Kresse B., Gmeiner J., Privalov A. F., Kruk D., Fujara F., & Rössler E. A. (2012). *Protracted Crossover to Reptation Dynamics: A Field Cycling ^{1}H NMR Study Including Extremely Low Frequencies*. Macromolecules, 45(3), 1408-1416.
[30] Meier R., Herrmann A., Hofmann M., Schmidtke B., Kresse B., Privalov A.F., Kruk, D., Fujara, F., & Rössler E.A. (2013). I*so-Frictional Mass Dependence of Diffusion of Polymer Melts Revealed by ^{1}H NMR Relaxometry.* Macromolecules, *46(14)*, 5538-5548.

/ APPLICATIONS

3.5 Heteronuclei

The possibility to perform multi-nuclear analysis extends the potential of FFC NMR Relaxometry and may prove important for characterization of certain materials or substances and to unlock molecular dynamics information of other key nuclei.

Up to now, most applications of NMR relaxometry involved the study of protons due to the low sensitivity of other nuclei (hetero-nuclei) and to technical difficulties mainly related to the signal-to-noise (S/N) ratio problems caused by the low acquisition frequency.

The technique of Fast Field Cycling allows the direct observation of hetero-nuclei with low receptivity and detectability, due to the fact that the magnetic field strength can be switched without the need to vary the frequency of the spectrometer.

This multi-nuclear approach expands the potential of Fast Field Cycling NMR applications and allows exploration of the field dependence of the spin-lattice relaxation time T_1 of important hetero-nuclei within substances, especially at low Larmor frequencies. This multi-nuclear approach expands the potential of Fast Field Cycling NMR applications and allows exploration of the field dependence of the spin-lattice relaxation time T_1 of important hetero-nuclei within substan- ces, especially at low Larmor frequencies, where other conventional NMR experiments present severe S/N ratio degradation.

The FFCR technique allows investigation of the content and/or the ability to characterize compounds containing important NMR-sensitive nuclei, such as ^{2}H, ^{7}Li, ^{13}C, ^{19}F, ^{31}P, ^{23}Na. The presence of such nuclei in a limited number of positions can be explored, therefore providing important structural information. The possibility of measuring nuclear spin relaxation, on nuclei other than ^{1}H, over a wide range of frequencies presents a new advance in the possible applications of TD-NMR and the possibility for new channels of research.

In the following, we show the applicability of FFC technique for the acquisition of the longitudinal relaxation rate ($R = 1/T_1$) as a function of the applied magnetic field strength of some important hetero-nuclei.

DEUTERIUM

In the pictures below, Deuteron T_1 decay curves of fuel cell membranes acquired directly on solid sample are shown. These curves present an evident multi-exponentiality particularly at low field.

The relaxation data at three different fields have been evaluated with discrete and continuos methods, using a two components traditional multi-exponential fitting (**FIG. 21**) as well as by means of a Laplace inversion algorithm (**FIG. 22**) in order to evaluate the distribution curve of T_1 (UPEN algorithm was used).

Deuteron FFC NMR Relaxometry has recently (in 2016) been applied for investigating molecular dynamics in molecular liquids and polymers [1].

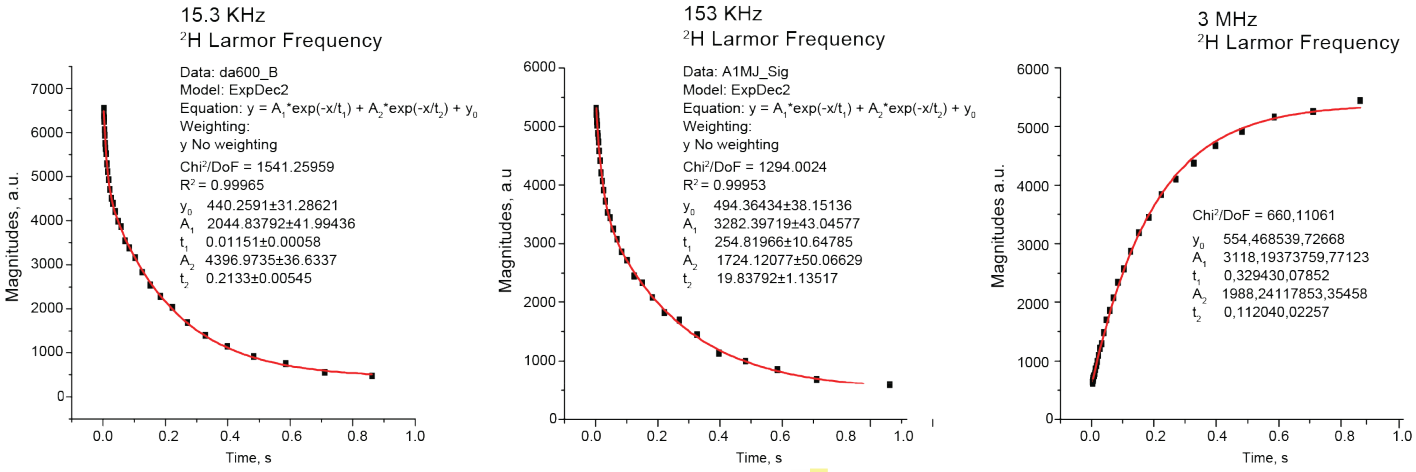

FIG. 21:
²H longitudinal relaxation data at different fields in fuel cell membranes fitted with a bi-exponential fitting algorithm.

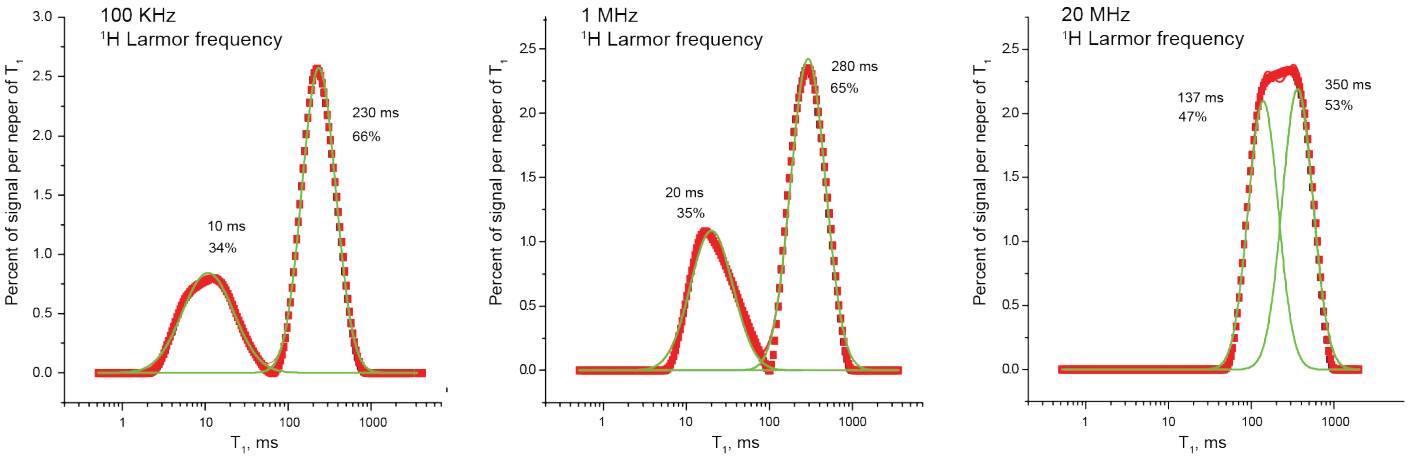

FIG. 22:
T_1 distributions obtained by means of a Laplace inversion algorithm at 3 different fields.

CARBON

In **FIG. 23** and **FIG. 24** examples of ^{13}C NMR acquisition at low field are reported, demonstrating the capacity of FFC NMR to investigate the relaxometric behavior of low NMR-sensitive nuclei at low magnetic field strengths.

In **FIG. 24**, it is shown the Longitudinal Relaxation Decay of a ^{13}C-enriched sample of a carboxylic acid that was measured by acquiring a ^{13}C NMR signal at the magnetic field strength of 2.35 mT (equivalent to 0.1 ^{1}H MHz) and at the temperature of -120 °C.

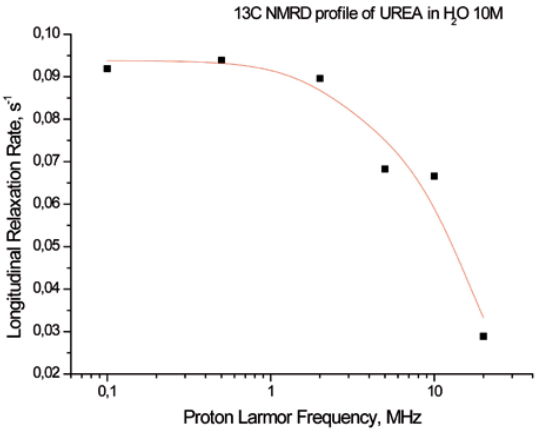

FIG. 23:
^{13}C NMRD profile of urea in water.

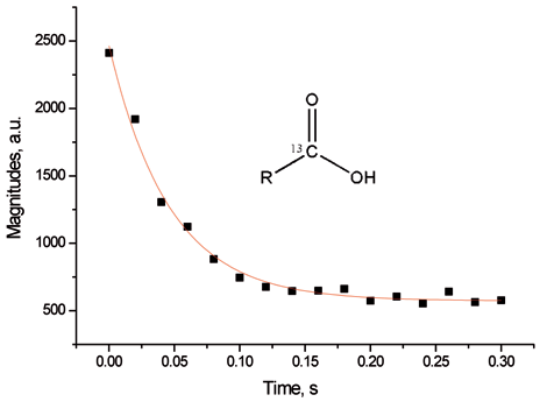

FIG. 24:
^{13}C NMR longitudinal decay curve of a carboxylic acid.

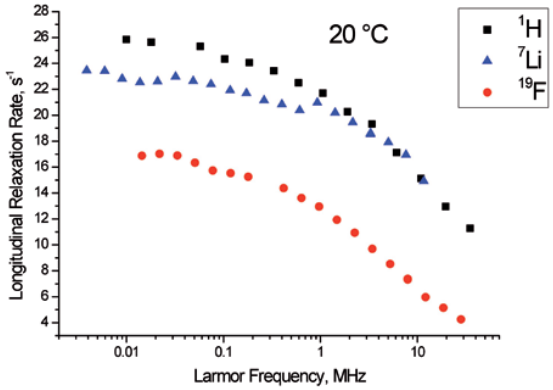

FIG. 25:
NMRD profiles of three different nuclei (^{1}H, ^{7}Li and ^{19}F), at 20°C, belonging to the same sample of an electrolyte solution for a battery system.

LITHIUM AND FLUORINE

Lithium is an important component of batteries in electronics industry. The fluorine nucleus is often found as part of the organic counter-ion of lithium-based electrolytes for batteries. The possibility to study the relaxation rates of these important nuclei could aid the studies for new battery electrolyte and electrode materials (**FIG. 25**). ^{19}F FFCR NMR has been applied to investigate the molecular dynamics of liquid crystals [2].

REFERENCES:

[1] Flämig M., Becher M., Hofmann M., Körber T., Kresse B., Privalov A.F.,Willner L., Kruk D., Fujare F & Rössler E.A. (2016). *Perspectives of Deuteron Field-Cycling NMR Relaxometry for Probing Molecular Dynamics in Soft Matter*. The Journal of Physical Chemistry B, 120(31), 7754-7766;
[2] Bubici S., Calucci L., Ferrante G. & Geppi M. (2012). *Collective and molecular motions of fluorinated liquid crystals by means of ^{19}F Fast Field-Cycling NMR relaxometry*. Chemical Physics Letters, 549, 27-31.